S4

X-RAY LAUE DIFFRACTION STUDY OF OXYGEN PRECIPITATES IN CZOCHRALSKI SILICON

J. Růžička, O. Caha and M. Meduňa

Department of Condensed Matter Physics, Faculty of Science, Masaryk University, Kotlářská 2, 611 37 Brno, Czech Republic
ruzmen@physics.muni.cz

In the presented article we study oxygen precipitates in annealed Czochralski silicon by means of X-ray diffraction in Laue geometry. Reflection and transmission curves obtained by measurement are compared with curves calculated using Takagi equations and statistical dynamical theory of diffraction. Parameters of the simulations are: relative volume and radii of defects, whose cores are formed by the oxygen precipitates and whose shape we assume to be spherical. Using these two parameters we calculate the absolute concentration of defects inside the crystal. We study the dependency of these parameters on pre-annealing at high temperature, on nucleation temperature and on duration of precipitation anneal.

Exended coontribution submitted.

S5

X-RAY DIFFRACTION ANALYSIS OF SURFACE SI NANOSTRUCTURES USED FOR Ge NANOHETEROEPITAXY

J. Matejova[1,2], G. Kozlowski[1], P. Zaumseil[1], V. Holy[2] and T. Schroeder[1]

[1]IHP, Im Technologiepark 25, D-15236 Frankfurt (Oder), Germany
[2]Faculty of Mathematics and Physics, Charles University, Ke Karlovu 5, 121 16 Prague, Czech Republic
matejova@ihp-microelectronics.com

Integrating low-defect Ge layers on Si substrate is of increasing interest due to its possible applications in optoelectronics and CMOS technologies. To avoid nucleation of dislocations caused by relatively large lattice mismatch between Si and Ge, nanoheteroepitaxy strain-relieving mechanism was suggested [1]. To prove the functionality of this mechanism, we investigate the strain field in Si line nanostructures covered by SiO_2 growth mask. By comparison of experimental XRD data with simulations (X-ray kinematical scattering theory), we refined the shape coordinates of the nanostructures taken from TEM images. We carried out a strain field simulation based on elasticity theory and showed insufficiency of conventional model of the strain in Si after thermal oxidation. Therefore we suggested an iterative evolutionary algorithm to determine the strain field from the experimental XRD data. Preliminary results, where we reached better agreement, are shown.

Exended coontribution submitted.

S6

DEFECT DETERMINATION IN EPITAXIAL a-PLANE GaN LAYERS

Mykhailo Barchuk,[a] Václav Holý,[a] Dominik Kriegner,[b] Julian Strangl,[b] Stephan Schwaiger,[c] and Ferdinand Scholz[c]

[a] Charles University in Prague, Czech Republic
[b] Johannes Kepler University, Linz, Austria
[c] Ulm University, Germany
E-mail: mikebarchuk@rambler.ru

Technological applications of optoelectronic devices based on (0001), i.e., c-oriented GaN are complicated by the piezoelectric effect along the [0001] direction. This phenomenon gives rise to a band bending, known as the quantum confined Stark effect [1].

Non-polar or semipolar GaN thin films overcome this problem. However, this type of material possesses a large number of defects, especially stacking faults (SF) so that a reliable method for the determination of the defect densities is of large importance.

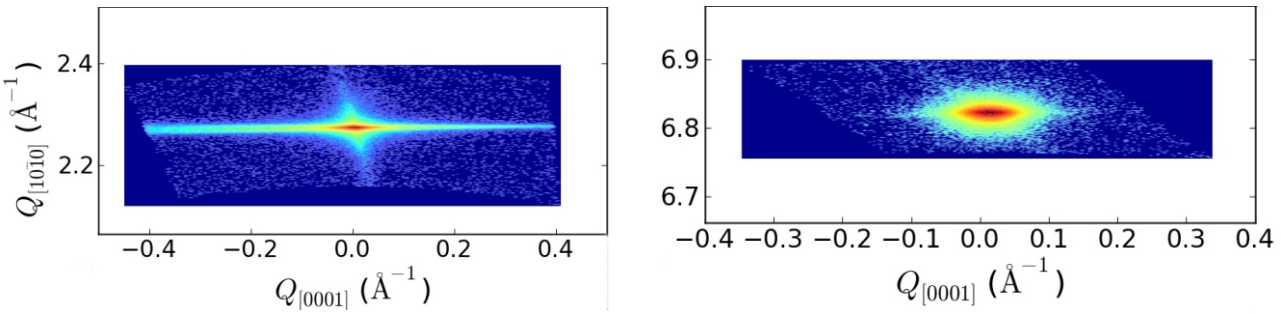

Figure 1. Example of the reciprocal space maps of x-ray diffuse scattering measured in the symmetric non-coplanar $(10\bar{1}0)$ (left) and $(30\bar{3}0)$ diffractions (right) from the sample with the lowest stacking fault densities.

We investigate non-polar a-plane oriented GaN epitaxial layers with the $(11\bar{2}0)$ surface orientation. In the layers of a-plane GaN, two types of basal plane stacking faults with the displacement vectors **R** = 1/6$(20\bar{2}3)$ and 1/3 $(1\bar{1}00)$ are the most typical defects [2]. Another defect types (extrinsic basal stacking faults with **R**=1/2(0001), prismatic stacking faults with **R**=1/2$(10\bar{1}1)$ can also occur but their formation energy is significantly higher so that one can neglect their influence [3].

For the detection of SFs by X-ray diffraction, the visibility criterion can be applied. If **g**.**R** n (**g** is the diffraction vector, n is an integer), the diffuse X-ray scattering from the SFs has the form of [0001]-oriented streaks perpendicular to the fault planes; if **g**.**R** = n the defects are generally invisible by X-ray diffraction [4]. In the latter case, (for example in $(30\bar{3}0)$ diffraction) a broadening of the diffraction maximum is observed caused by another defects such as dislocations, wafer curvature, and surface roughness.

We investigated a series of 4 samples grown by MOVPE technique [5] with various densities of stacking faults.

The X-ray diffraction (XRD) measurements were performed using a custom built rotating anode setup. A double bent parabolic multilayer mirror and a Ge(220) channel cut monochromator were used to produce a parallel beam of CuK $_1$ radiation. The diffracted radiation was measured by a linear multichannel detector.

The reciprocal space maps of diffracted intensity were measured in a non-coplanar Bragg geometry. In order to reach the diffractions $(10\bar{1}0)$ and $(20\bar{2}0)$, in which the visibility criterion is fulfilled, and using the scattering plane containing the [0001] streak direction, this scattering plane had to be tilted by 30 deg with respect to the surface normal. In this tilted plane, diffractions $(10\bar{1}0)$ and $(20\bar{2}0)$ are symmetric. In $(10\bar{1}0)$ and $(20\bar{2}0)$ diffractions we were able to observe the [0001]-streaks arising from the various types of SFs (Fig.1). For comparison, we measured also the reciprocal space maps in $(30\bar{3}0)$, where the visibility criterion is not fulfilled. In this diffraction, the SF-related streak does not appear indeed (Fig.1, the right panel).

All the measured diffraction maxima are broader than expected from the estimated instrumental broadening. However, since we are interested in the shape of the peaks far from the sharp central peak, the resolution function does not influence our analysis.

Our model of simulation enables to calculate the profiles along the streaks in any diffraction. As input parameters we use the density of SFs, the coherence width of the primary beam and the shape factor of the coherence function in direct space. Using the Monte Carlo method we generate the positions of defects as a random Markov-like sequence. Then, we compute the displacement field caused by defects, and finally applying the kinematical approximation we obtain the intensity distribution along the [0001] direction in reciprocal space.

Comparison of the measured intensity distributions along the streaks with simulations supposing allows us to determine the prevailing displacement vector ***R*** of the SFs and their density. Depending on the sample growth mode the total densities vary between 10^5– 10^6 cm^{-1}.

1. F. Bernardini, V. Fiorentini, and D. Vanderbilt, Rhys. Rev. B **56,** R10024 (1997).
2. D.N. Zakharov, Z. Liliental-Weber, B. Wagner, Z.J. Reitmeier, E.A. Preble, and R.F. Davis, Phys Rev. B **71**, 235334 (2005)
3. M.A. Moram, C.F. Johnston, J.L. Hollander, M.J. Kappers, and C.J. Hupmhreys, *Physica B*, **404**, 2189-2191 (2009**).**
4. P. Hirsch, A. Howie, R. Nicholson, D.W. Pashley and M.J. Whelan, Electron Microscopy of Thin Crystals, Krieger Publishing Company, Malabar, Frorida (1977).
5. S. Schwaiger, F. Lipski, T. Wunderer, and Ferdinand Scholz, Phys. Status Solidi C **7**, No. 7-8, 2069-2072 (2010).

This work has been supported by the Grant Agency of Charles University in Prague (projects SVV 263307 and 22310).

S7

STUDY OF MN INTERSTITIALS IN (Ga,Mn)As USING HRXRD

L. Horák[1], J. Matějová[1], X. Martí (a)[1], V. Holý[1], V. Novák[2], Z. Šobáň[2,3], S. Mangold[4], and F. Jimenez-Villacorta[5]

[1]Department of Condensed Matter Physics, Charles University, Prague, Czech Republic
[2]Institute of Physics ASCR, Prague, Czech Republic
[3]Department of Microelectronics, The Czech Technical University in Prague, Czech Republic
[4]Karlsruhe Institute of Technology, Karlsruhe, Germany
[5]Department of Chemical Engineering, Northeastern University, Boston, USA
horak@karlov.mff.cuni.cz

The (Ga,Mn)As, belonging to the diluted magnetic semiconductors, is intended for a spintronics application, but the temperature of the magnetic ordering is decreased among others due to the presence of the interstitial Mn. The amount of the interstitials can be reduced by the post-growth annealing [1], which leads to the out-diffusion of the interstitials to the free surface. Although this material has been intensively studied for last decade, the process of the out-diffusion is not yet fully understood [1–2].

We present a method for the determination of the concentration depth profiles of Mn interstitial ions in (Ga,Mn)As thin epitaxial layers using high-resolution x-ray diffraction (HRXRD) [3]. The measured diffraction curves for several diffraction maxima *hkl* were fitted to the theoretical curves based on standard dynamical diffraction theory (figure 1). From the asymmetry of the intensities of the thickness fringes it is possible to characterize an eventual depth inhomogeneity of the interstitial density in the (Ga,Mn)s layer. The depth profiles of the Mn interstitial density obtained for the sample in various annealing states were compared to the numerical drift-diffusion simulations, from this comparison the diffusivity of the interstitials in (Ga,Mn)As host lattice can be estimated.

The epitaxial GaMnAs layers under study were grown on (001)GaAs substrates by molecular beam epitaxy. A nondestructive character of the characterization (in contrast for instance to the transmission electron microscopy) allows to investigate the same sample in various annealing states. We measured an as-grown sample, then after 24 hours of annealing in the air at 160°C and finally after 20 cycles of etching and short annealing (under the same conditions as in the previous case). We have determined the depth profiles of the interstitial density for all samples and these have been compared to the numerical simulations of the interstitial drift-diffusion in the sample.

From these comparisons the diffusivity of the Mn ions in the (Ga,Mn)As lattice has been estimated (figure 2). The results show that the flux of the Mn ions towards the free surface is strongly affected by the internal electric field produced by inhomogeneously distributed holes [4].

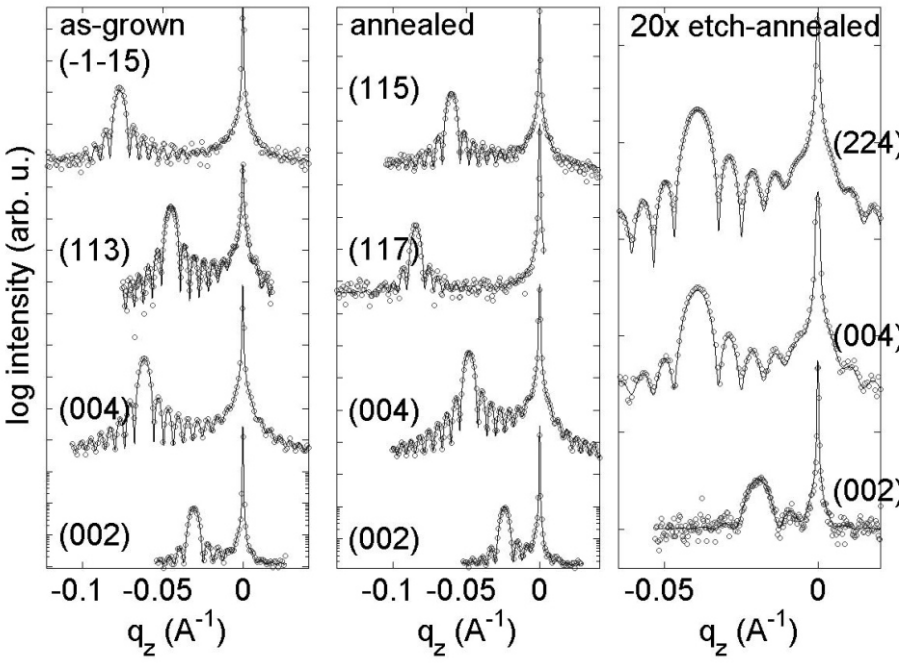

Figure 1. The measured diffraction curves (circles) for as-grown, annealed and re-annealed (sequentially 20x etched and annealed) sample with their theoretical fits (solid line).

1. K. W. Edmonds, P. Bogus lawski, K. Y. Wang, R. P. Campion, S. N. Novikov, N. R. S. Farley, B. L. Gallagher, C. T. Foxon, M. Sawicki, T. Dietl, M. Buongiorno Nardelli, and J. Bernholc, Phys. Rev. Lett. 92, 037201 (2004).
2. J. Adell, I. Ulfat, L. Ilver, J. Sadowski, K. Karlsson, and J. Kanski, Journal of Physics Condensed Matter 23, 085003 (2011).
3. L. Horák, Z. Šobáň, and V. Holý, Journal of Physics: Condensed Matter 22, 296009 (2010).
4. L. Horák, J. Matějová, X. Martí, V. Holý, V. Novák, Z. Šobáň, S. Mangold, and F. Jiménez-Villacorta, Phys. Rev. B – *accepted for publishing.*

This work is a part of the research programme MSM 0021620834 financed by the Ministry of Education of the Czech Republic. The work has been supported by the European Community's Seventh Framework Programme NAMASTE under grant agreement number 214499. The XANES experiment was carried out at synchrotron ANKA, Germany.

Extended contribution submitted.

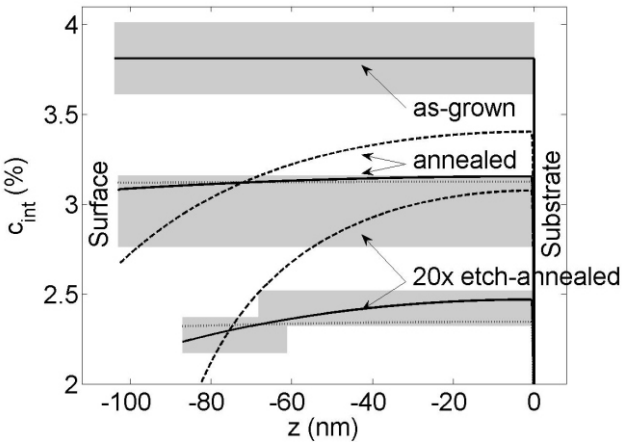

Figure 2: Depth profiles of the concentration of the Mn interstitials in as-grown sample, annealed and 20x etch-anneled. The concentration profiles determined by HRXRD are represented by gray areas indicating the uncertainty of the profiles. The profiles obtained from the diffusion simulations for the interstitial diffusion constant $D_n = 4 \times 10^{-20}$ m^2/s are plotted by solid lines; the concentration profiles simulated for 10 times larger and 10 times smaller values of the Mn diffusion constant are plotted by dotted and dashed lines, respectively. The initial concentration profile for all simulations is given by the concentration of Mn interstitials in as-grown sample.

S8

QUANTUM DOTS IN AMORPHOUS MATRIX

J. Endres[1], S. Daniš[1], V. Holý[1], M. Mixa[1], V. Valeš[1], M. Buljan[2]

[1]*Department of Condensed Matter Physics, Charles University, Prague, Czech Republic*
[2]*Rudjer Boskovic Institute, Zagreb, Croatia*
jan.endres@seznam.cz

Systems of quantum dots (QDs) in amorphous matrix are intensively studied because of their prospective technological applications. Their advantages are tunable electrical properties depending on the size, like band gap, electro/photoluminescence, high optical nonlinearity or charge storage for a long time. Thus it can be used in lasers, solar cells, photodetectors , high-speed memories and other optoelectronic devices. Metal QDs in amorphous matrix are recently investigated as well, namely due to interesting magnetic behavior (superparamagnetism, for example). Regularity of QDs system and uniformity of QDs sizes is important for good physical properties.

Ordering of QDs originates in preferential nucleation of QDs in minima of chemical potential on the surface, which correspond with surface energy, during the growth. In the case of QDs in crystalline matrix is ordering caused by elastic forces originated from mismatch of lattice constants of materials in adjacent layers. On the oder hand amorphous matrix ordering is obtained due to diffusion and surface morphology. In such system QDs are ordered into crystal-like lattice only in small blocks, see [1, 2]. Nearly periodic arrangement of QDs in the entire multilayer can be achieved by ion beam irradiating, when the sample is irradiated by ion beam under given angle and the places of ions flyby become a nucleations centers, see [3, 4].

We will study the structure of QDs systems (size, shape, ordering in matrix). X-ray scattering methods are suitable for this purpose. These methods are nondestructive and irradiated volume is large so we obtain averaged information from many irradiated dots. We will primarily use x-ray diffraction, reflectivity and possibly GISAXS. We can use other method like TEM, but it is destructive method, in which the sample is destroyed at preparation for experiment. Ordering of QDs in (SiO_2 + Ge)/SiO_2 multilayers was studied by M. Buljan et al., see [1-4], ordering of QDs in (SiO_2 + Ni)/SiO_2 multilayers is studied recently.

Growth of QDs multilayer can be simulated via kinetic Monte Carlo method (KMC). In [5] KMC was used for growth of QDs in a crystalline matrix. Each QDs layer was created on atomically flat wetting layer (WL). Chemical potential was in form

where x is point on surface, $_0$ is reference value of chemical potential, w is the volume density of elastic energy, is the surface tension, is the surface curvature and V_0 is the atomic volume. Due to atomically flat WL the third term is zero and the chemical potential is affected only by elastic energy as mentioned above. We modified this approach for

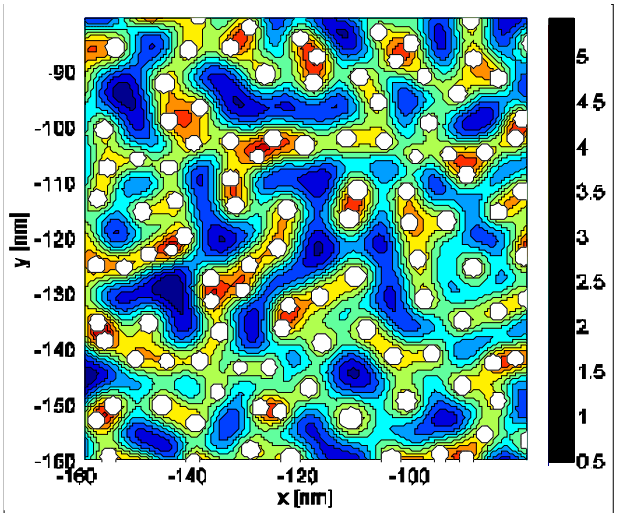

Figure 1. Positions of QDs in the part of the first layer and height of surface above them.

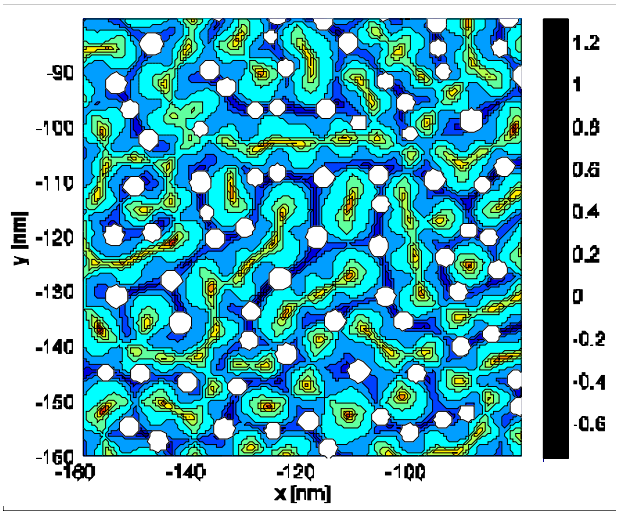

Figure 2. Positions of QDs in the part of the second layer and curvature of surface below them. The QDs lie in the valleys on the surface, i.e. in the minima of the surface energy.

simulating the growth of QDs in amorphous matrix. In this case the second term in equation (1) is zero and chemical potential is affected only by the third term. Surface shape of covering layer above one QD is approximated by Gauss function, see [1]. For the whole surface with index j_3 we use equation

$$h_{j3}(x) \quad \sum_{j_1,j_2} f(x \quad X_{j_1,j_2,j_3\ 1}) \quad Cf(x \quad X_{j_1,j_2,j_3\ 2}) , \quad (2)$$

where j_1 and j_2 are indices which describe positions of dots in the layer j_3 and f denotes Gauss function

$$f(x) \quad \exp \quad \frac{x^2}{2^{\ 2}} \quad (3)$$

with full width at half maximum and C is a factor, which determines the contribution of layer with index $j_3 - 2$. Preliminary results of simulation show, that QDs in second layer are preferentially created in the minima of surface height, i.e. in places with minimal curvature, see Figure 1 and 2.

1. M. Buljan, U. V. Desnica, M. Ivanda, N. Radić , P. Dubček, G. Dražić, K. Salamon, S. Bernstorff, and V. Holý, *Physical Review B*, **79**, (2009), 035310.
2. M. Buljan, U. V. Desnica, G. Dražić, M. Ivanda, N. Radić, P. Dubček, K. Salamon, S. Bernstorff, and V Holý, *Nanotechnology*, **20**, (2009) 085612.
3. M. Buljan, I. Bogdanović -Radović, M. Karlušić, U. V. Desnica, G. Dražić, N. Radić, P. Dubček, K. Salamon, S. Bernstorff, and V. Holý, *Appl. Phys. Lett.*, **95**, (2009), 063104.
4. M. Buljan, I. Bogdanović-Radović, M. Karlušić, U. V. Desnica, N. Radić, N. Skukan, G. Dražić, M. Ivanda, O. Gamulin, Z. Matej, V. Valeš, J. Grenzer, T. W. Cornelius, H. T. Metzger, and V. Holý, *Physical Review B*, **81**, (2010), 085321.
5. M. Mixa, V. Holý, G. Springholz, and G. Bauer, *Physical Review B*, **80**, (2009), 045325.